Civil Engineering and Architecture 10(7): 2833-2846, 2022
DOI: 10.13189/cea.2022.100704 http://www.hrpub.org

Flood Modelling due to Dam Failure Using HEC-RAS 2D with GIS Overlay: Case Study of Karalloe Dam in South Sulawesi Province Indonesia

Riswal Karamma[1,*], Sugiarto Badaruddin[2], Rifaldi Mustamin[1], Zubair Saing[3]

[1]Department of Civil Engineering, Hasanuddin University, P.O. Box 90245, South Sulawesi, Indonesia
[2]Department of Civil Engineering, Politeknik Negeri Ujung Pandang, P.O. Box 90245, South Sulawesi, Indonesia
[3]Department of Civil Engineering, Universitas Muhammadiyah Maluku Utara, Ternate City, Indonesia

Received August 12, 2022; Revised September 17, 2022; Accepted September 26, 2022

Cite This Paper in the Following Citation Styles

(a): *[1] Riswal Karamma, Sugiarto Badaruddin, Rifaldi Mustamin, Zubair Saing , "Flood Modelling due to Dam Failure Using HEC-RAS 2D with GIS Overlay: Case Study of Karalloe Dam in South Sulawesi Province Indonesia," Civil Engineering and Architecture, Vol. 10, No. 7, pp. 2833 - 2846, 2022. DOI: 10.13189/cea.2022.100704.*

(b): *Riswal Karamma, Sugiarto Badaruddin, Rifaldi Mustamin, Zubair Saing (2022). Flood Modelling due to Dam Failure Using HEC-RAS 2D with GIS Overlay: Case Study of Karalloe Dam in South Sulawesi Province Indonesia. Civil Engineering and Architecture, 10(7), 2833 - 2846. DOI: 10.13189/cea.2022.100704.*

Copyright©2022 by authors, all rights reserved. Authors agree that this article remains permanently open access under the terms of the Creative Commons Attribution License 4.0 International License

Abstract A dam is one of the water structures that have many benefits for humans. However, flood disasters caused by dam break may have a very bad impact on human life. This study specifically analyzed the impact of flooding caused by the failure of the Karalloe dam in Bone Regency, South Sulawesi Province, Indonesia. For the first time, the selected flood discharge used in the dam break analysis was verified using the Creager graph by comparing the calculated discharge from several synthetic unit hydrograph methods (HSS) with the flood discharge measured on the automatic water level recorder (AWLR) at the monitoring point. The impact of flooding due to dam break was simulated using HEC-RAS 2D combined with ArcGIS for mapping. The calculation results of the design flood discharge based on rainfall data using the methods of HSS Nakayasu, HSS ITB I, HSS ITB II, and HSS SCS (HEC-HMS) as well as the calculation of the designed flood discharge based on the discharge data showed that the design flood discharge value which is closest to the measured discharge value and Q1000 Creager was the HSS SCS method. The flood discharge values obtained based on the HSS SCS method for Tr (return period) 2 years, Tr 5 years, Tr 10 years, Tr 20 years, Tr 25 years, Tr 50 years, Tr 100 years, and Tr 1000 years were 322.70 m^3/s, 464.10 m3/s, 560.40 m^3/s, 658.40 m^3/s, 682.70 m^3/s, 787.00 m^3/s, 885.70 m^3/s, and 1202.60 m^3/s, respectively. The simulation results showed that 22 villages will be affected by flooding due to the failure of the Karalloe dam and the fastest standby time of the flood is 12 minutes, namely at Lookout Point 7 in Paitana Village. This result suggests that early warning system should be installed at the downstream of the dam and flood disaster mitigation should be adopted and applied to these threatened area.

Keywords Flood Modelling, Dam Break, Synthetic Unit Hydrograph, HEC-RAS 2D

1. Introduction

The dam is a piece of infrastructure beneficial to human life by promoting social and economic development. Dams serve many purposes, including irrigation, power generation, water supply, flood control, fishing, and recreation [1,2]. The Karalloe Dam is a rock-fill type with a concrete membrane and side spillway without a door with a maximum storage volume of 40.53 million m^3, which is used to meet water needs for irrigation of Kelara-Karalloe, covering an area of 7004 ha and is expected to be developed for hydropower potential of 4.5 MW, flood control (64.17 m^3/s), conservation of water resources, and tourism development [3-5].

In addition to their numerous advantages, dams pose a

significant risk of disaster in the event of a failure or collapse, which can result in loss of life and property as well as the destruction of existing infrastructure in the downstream area [6,7]. The construction of a dam is frequently followed by the development of communities in the downstream area, which increases the risk of dam failure [8]. Dams can break or collapse due to overtopping, the overflow of water through the dam's top, causing erosion and landslides in the dam's body, particularly in embankment dams. The dam's failure will result in flash floods, in which the water stored in the dam will flow downstream with a giant flood discharge and at high speed [9].

Because of the conditions affecting dam stability and retention efficiency, a greater spread of awareness about risk factors affecting dam safety is required [9]. Some negative factors include damaging spillway capacity that cannot drain flood discharge due to changes in weather patterns effectively and exacerbated extreme climates [10,11]. These factors can increase the risk of flooding in downstream areas due to dam failure, which is exacerbated by increased exposure to human settlements and the potential for high flood susceptibility [12]. Given the possibility of disasters caused by a dam collapse in response to conditions downstream of the dam, flood simulations are required to predict areas that will be affected downstream of the dam, particularly in a dam collapse [13].

This significant potential danger necessitates the creation of a detailed and effective emergency action plan (EAP). In general, dam break analysis is the primary input of EAP [14]. The source of data for compiling this EAP is the result of dam break analysis in the form of dam collapse simulation results [14]. In most downstream flood simulations caused by a dam failure, it is assumed that the dam collapses completely and unexpectedly [15]. Kheirkhah et al. [16], SMPDBK [17], FLDWAV [16], and HEC-RAS can be used to model water flow due to dam collapse [18]. Among the many applications available, the 2D numerical model HEC-RAS is ideal for determining water depth, inundation area, flow velocity, and water level profile in two dimensions [19].

The Karalloe Dam itself was scheduled to begin construction in 2012, continued to be built in 2017, and completed in 2021. The Karalloe Dam is located in Garing Village, Datara Village, and Taring Village, Gowa Regency, South Sulawesi Province. This location is located approximately 137 km to the southeast of Makassar City. Karalloe Dam is a large dam which is one of the assets belonging to the Government of the Republic of Indonesia [4]. The dam with a maximum storage volume of 40.53 million m^3 is one of the National Strategic Projects with a high level of risk and potential danger. On January 22, 2019 there was a flood at the Karalloe Dam. This flood resulted in water from the Kelara River being able to pass through the coffer dam which was made to hold water. Mitigation of the possibility of a dam failure is very necessary to be done as an effort to prevent the occurrence of large losses both in terms of human and material casualties.

Flood simulations due to the collapse of the Karalloe dam were performed in this study using HEC-RAS 2D and combined with ArcGIS for mapping. For the first time, the flood discharge used in the dam break analysis was verified using the Creager graph by comparing the calculated discharge from several synthetic unit hydrograph methods (HSS) with the flood discharge measured on the automatic water level recorder at the monitoring point. A flood flow pattern will be obtained from the simulation results, which will then be followed by flood tracing in flood-prone locations to serve as a guide for dam managers and governments in the affected areas to prepare anticipatory steps in the event of an emergency condition at the dam.

2. Materials and Method

2.1. Materials

Several data sets are required to carry out this research, including (1) TRMM rainfall data (Tropical Rainfall Measuring Mission). The National Institute of Aeronautics and Space obtained rain data from 1998 to 2020 (23 years) (LAPAN); (2) Karalloe Dam technical data in general, primary dam body, and spillway building data to determine dam characteristics; (3) The reservoir capacity curvature describes the reservoir in the reservoir that is used in the flood track; (4) For flood tracking, topographic and bathymetric data were combined with DEMNAS (National Bathymetry and Digital Elevation Model) with an 8.3 m spatial resolution. (5) Pompengan-Jeneberang river basin authority (BBWSPJ) soil type map from 2018. (6) The Geospatial Information Agency provided a map of the 2019 Land Use Pattern.

2.2. Flood Discharge Design

Flood discharge analysis is used to determine flood discharge design based on data from current conditions. The availability of flow data determines the method for designing flood discharge analysis. Because flow data is not available, the flood discharge in this study is calculated by converting rain into the flow [20]. The design flood analysis was carried out using a synthetic unit hydrograph based on previous research that revealed that the HSS SCS method (HEC-HMS Application) was the closest to the Likupadde AWLR discharge and Crager Graph [21].

Data on land use, soil type, river topography, and TRMM rainfall were used in the hydrological analysis using the HEC-HMS application. TRMM is used in this study because it performs well for Indonesian territory and correlates with average daily rainfall observation data of

0.90 derived from various satellite rainfall data sources [22].

2.3. Dam Break Analysis

The HEC-RAS 2D application was used to simulate the failure of the Karalloe Dam. In this case, an evaluation is also performed to determine whether flooding from the most recent rainfall can cause overtopping at the dam's top. Table 1 shows technical information about the Karalloe Dam.

Fractures usually occur prior to the dam's total collapse (Figure 1). The following is Froehlich's [23] regression equation for average fracture width and failure time:

$$B_{ave} = 0.27\, K_0 . Vw^{0.32} . hb^{0.04} \quad (1)$$

$$tf = 63.2 \sqrt{\frac{Vw}{ghb^2}} \quad (2)$$

Where, B_{ave} = The average width of the fracture (m)

K_o = Constant (1.3 for overtopping collapse)

Vw = Storage volume at collapse (m^3)

Hb = Final height of fracture (m)

g = Gravity constant (9,80665 m/s^2)

tf = Collapse time (detik)

According to Froechlich [23], the mean side slope for overtopping failure should be horizontal to vertical (1:1).

2.4. Flood Mapping and Tracking

The flood simulation results from dam failure will be mapped using ArcGIS 10.8 software to identify flood-prone areas, which will then be classified based on a specific depth. Following the flood mapping, flood identification was performed to determine the affected location's distance from the dam, the depth of the flood, and the time of flood concentration from the dam to flood-prone locations.

Table 1. Technical data of Karalloe Dam

River's name	**: Karalloe**
Watershed area	: 195 km^2
Inundation area	: 145 Ha
Maximum storage volume	: 40.53 million m^3
Effective storage volume	: 29.50 million m^3
Off storage volume	: 11.03 million m^3
Flood water level	: + 252.40 m
Normal water level	: + 248.50 m
Low water level	: + 220.50 m
Type of dam	: Concrete membrane Stone backfill
Height of the dam from the foundation's base	: 82 m
Top elevation of dam	: + 253.00 m
Dam crest height	: 396 m
Dam crest width	: 10 m (Hot mix)
Spillway type	: Ogee
Overflow type	: Side overflow without door
Threshold elevation	: + 248.50 m
Overflow width	: 100 m

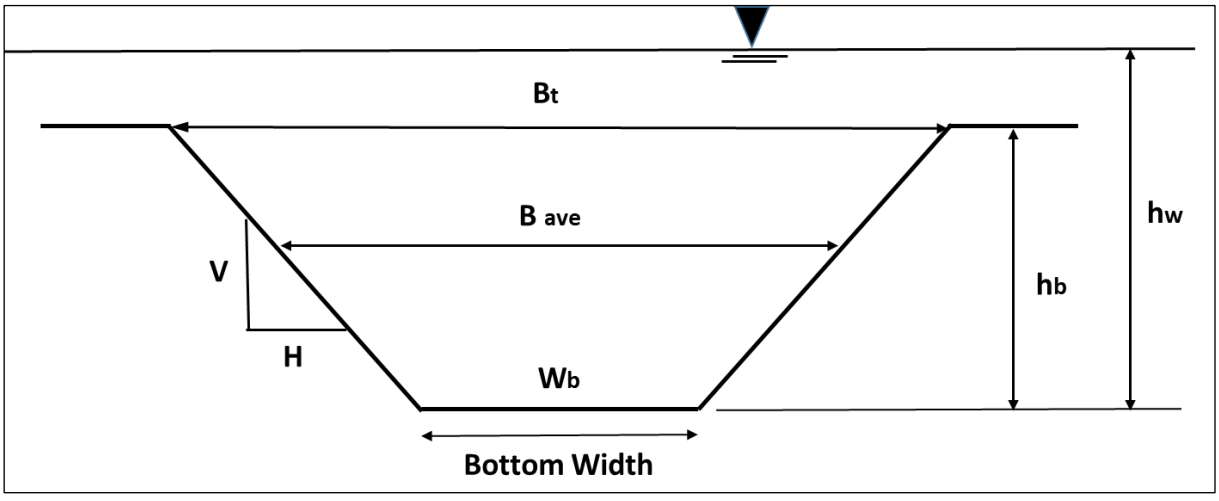

Figure 1. Fracture parameter overview

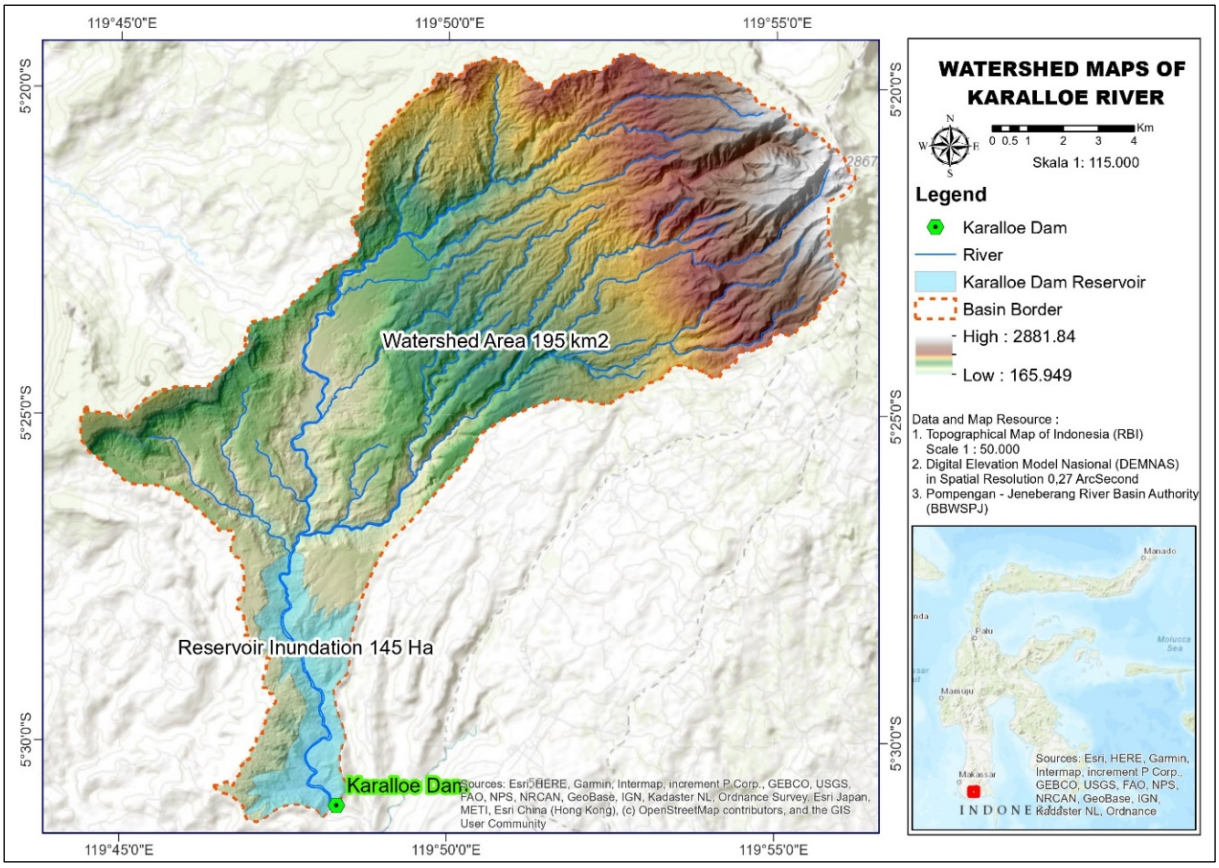
119°45'0"E
119°50'0"E
119°55'0"E
5°20'0"S
5°25'0"S
5°30'0"S
Watershed Area 195 km2
Reservoir Inundation 145 Ha
Karalloe Dam
WATERSHED MAPS OF KARALLOE RIVER
N
W
E
S
0 0.5 1 2 3 4 Km
Skala 1: 115.000
Legend
Karalloe Dam
River
Karalloe Dam Reservoir
Basin Border
High : 2881.84
Low : 165.949
Data and Map Resource :
1. Topographical Map of Indonesia (RBI) Scale 1 : 50.000
2. Digital Elevation Model Nasional (DEMNAS) in Spatial Resolution 0,27 ArcSecond
3. Pompengan - Jeneberang River Basin Authority (BBWSPJ)
Manado
Palu
Mamuju
Makassar
Sources: Esri, HERE, Garmin, Intermap, increment P Corp., GEBCO, USGS, FAO, NPS, NRCAN, GeoBase, IGN, Kadaster NL, Ordnance Survey, Esri Japan, METI, Esri China (Hong Kong), (c) OpenStreetMap contributors, and the GIS User Community

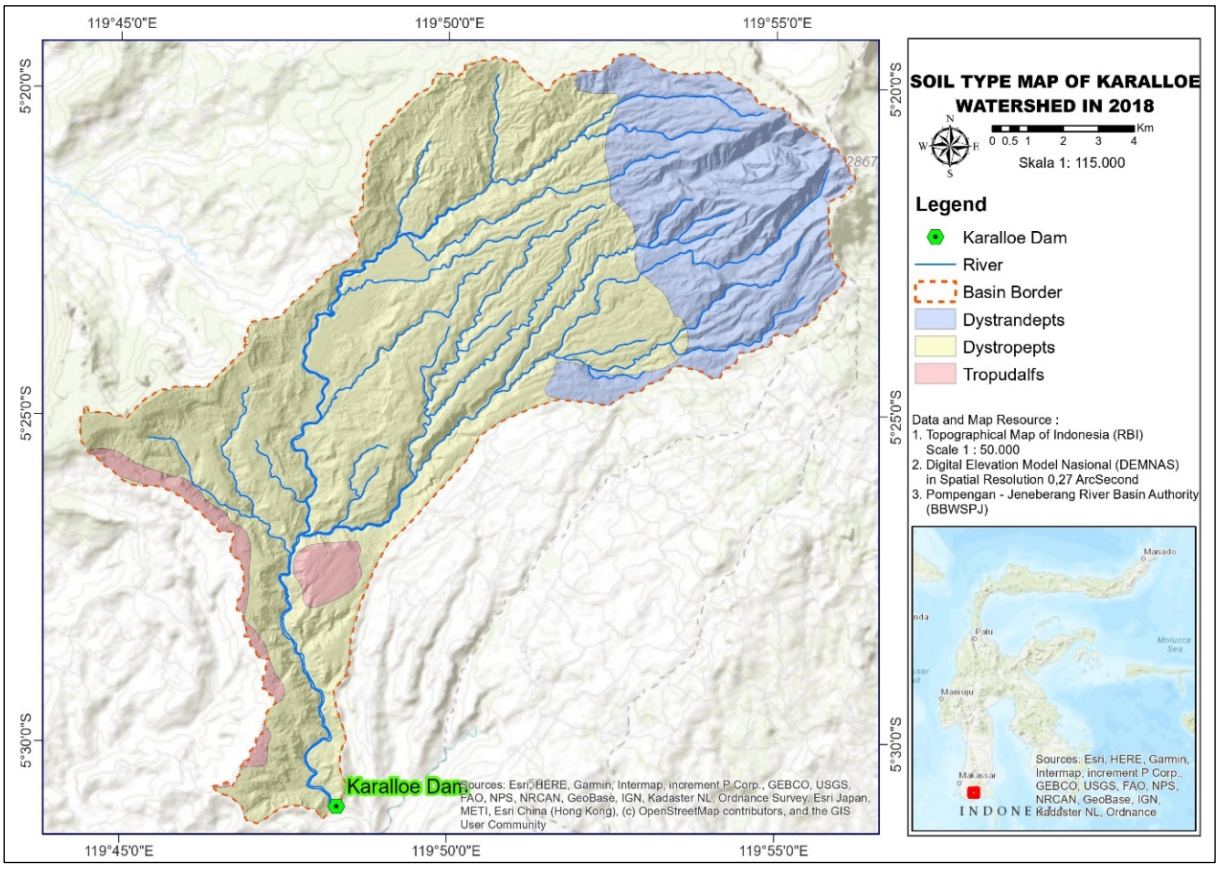
119°45'0"E
119°50'0"E
119°55'0"E
5°20'0"S
5°25'0"S
5°30'0"S
Karalloe Dam
SOIL TYPE MAP OF KARALLOE WATERSHED IN 2018
N
W
E
S
0 0.5 1 2 3 4 Km
Skala 1: 115.000
Legend
Karalloe Dam
River
Basin Border
Dystrandepts
Dystropepts
Tropudalfs
Data and Map Resource :
1. Topographical Map of Indonesia (RBI) Scale 1 : 50.000
2. Digital Elevation Model Nasional (DEMNAS) in Spatial Resolution 0,27 ArcSecond
3. Pompengan - Jeneberang River Basin Authority (BBWSPJ)
Manado
Palu
Mamuju
Makassar
Sources: Esri, HERE, Garmin, Intermap, increment P Corp., GEBCO, USGS, FAO, NPS, NRCAN, GeoBase, IGN, Kadaster NL, Ordnance Survey, Esri Japan, METI, Esri China (Hong Kong), (c) OpenStreetMap contributors, and the GIS User Community

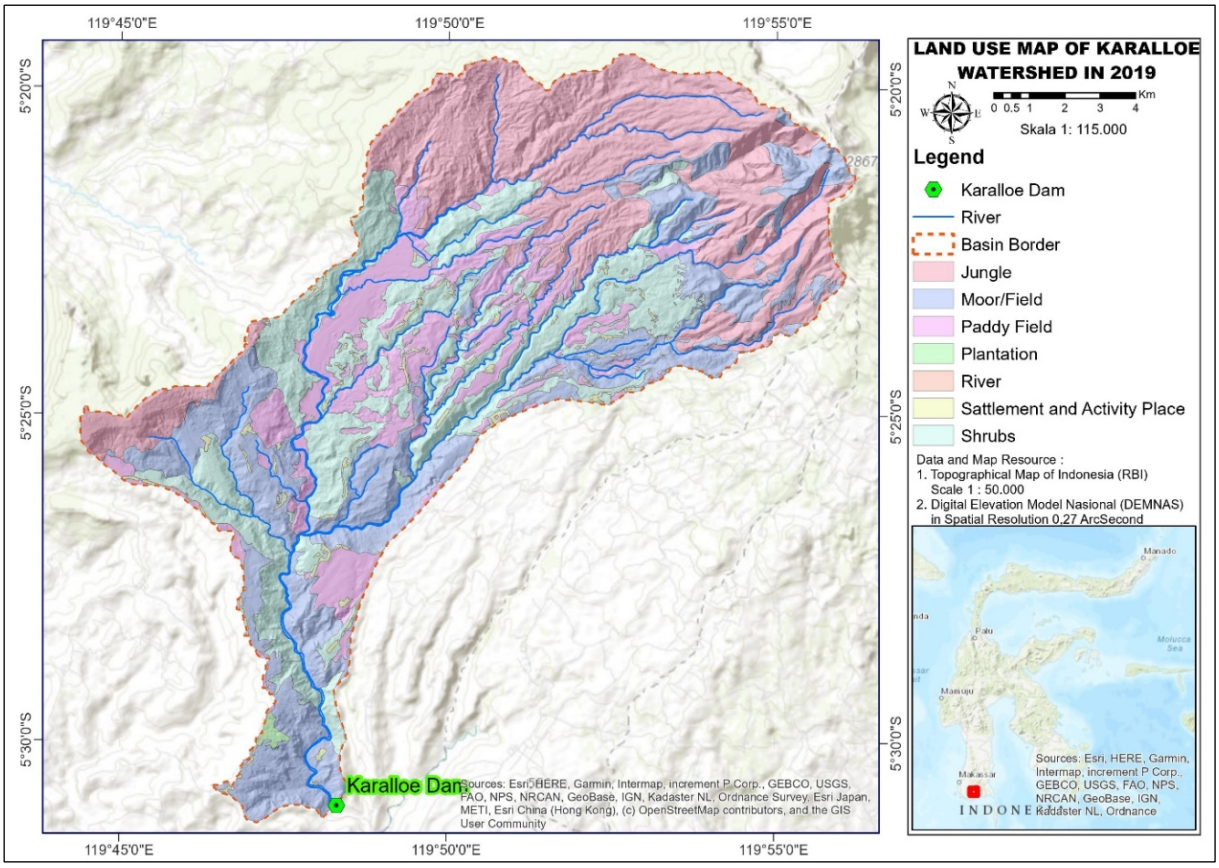

Figure 2. Map of Topographic, soil type and land use of the Karalloe Watershed

Table 2. HEC - HMS Input Parameters

Physical Parameters	Value
Watershed Area (km^2)	195,23
Initial Abstraction (mm)	23,40
Impervious (%)	0,58
Curve Number (CN)	68
Lag Time (min)	124,17

3. Results and Discussion

3.1. Karalloe Dam Design Flood Discharge

Based on the Karalloe Dam's design data, a QPMF (i.e., flow discharge for the Probable Maximum Flood) of 2,020 m^3/s was obtained in 2012, while the results of other researchers' analyses of the Karalloe Dam obtained a QPMF of 3307 m^3/s in 2017 [4]. It is necessary to analyze flood discharge using the most recent rainfall data to determine the increase in flood discharge, with the most significant discharge used as input for simulation to determine the impact of the Karalloe Dam failure.

Data on watershed characteristics such as topography, land use, and soil type are derived from the hydrological analysis using the SCS method (i.e., HEC-HMS) because they significantly impact rainwater that will become surface runoff. The map in Figure 2 can describe the characteristics of the Kelara watershed.

The characteristics of the Karalloe watershed can be seen in Figure 2, which shows that the watershed area is 195.23 km^2, the length of the main river is 27.27 km, the highest elevation is +848 masl, the lowest elevation is +165 masl, the average river slope is 0.026 percent, dystropepts dominate the soil type, and the land is dominated by forest. The input parameters for the HEC-HMS are derived from the results of the watershed characteristics analysis. Table 2 displays these parameters. Three TRMM posts collect rainfall data, which affects the Karalloe watershed. Figure 3 and Table 3 show the TRMM location and data.

The Probable Maximum Precipitation (PMP) analysis performed at the Karalloe Dam location yielded a value of 478.77 mm/day. In addition, a QPMF discharge analysis was performed using the HEC-HMS application, yielding a value of 3534.8 m^3/sec. Figure 4 depicts the outcome of the QPMF discharge analysis.

3.2. Simulation of Dam Failure

In this study, data are required to support the simulation to run HEC-RAS 6.0.1 and obtain the results of the dam collapse analysis. Figures 5 and 6 show the primary data and scenarios used in general.

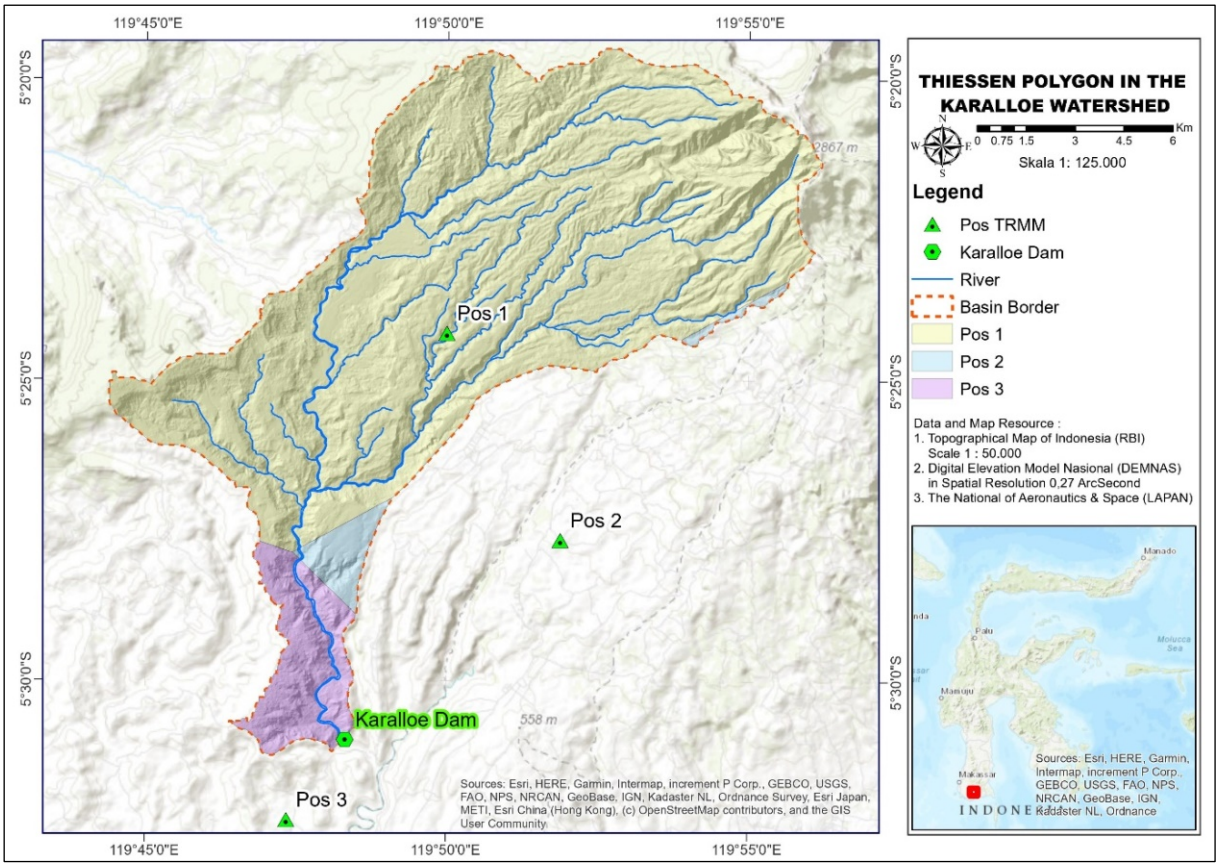

Figure 3. Thiessen polygon of the Karalloe watershed

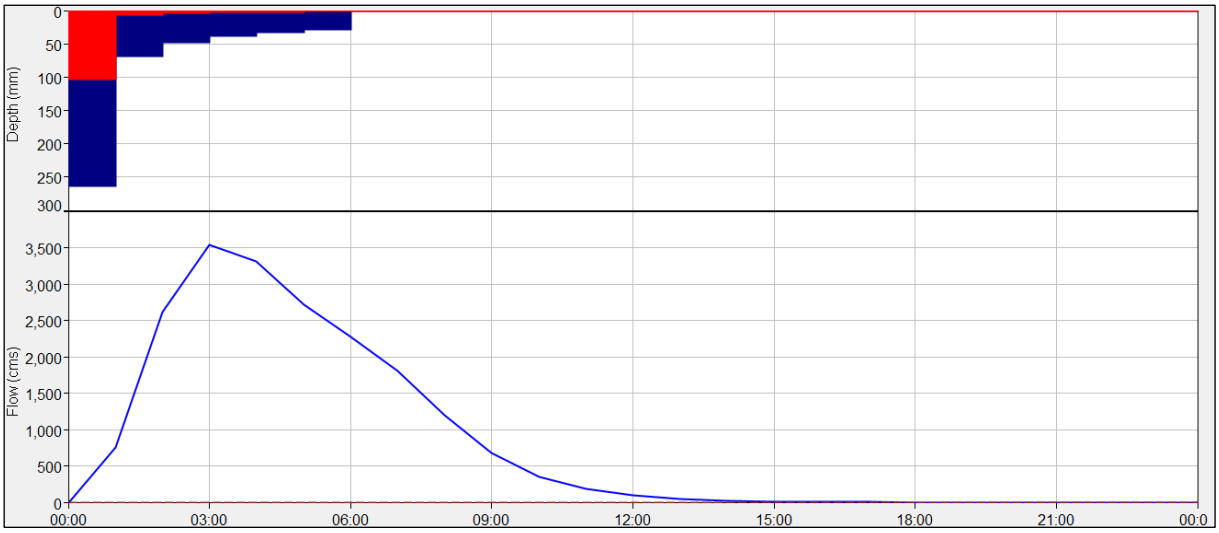

Figure 4. QPMF flood hydrograph of the Karalloe Watershed

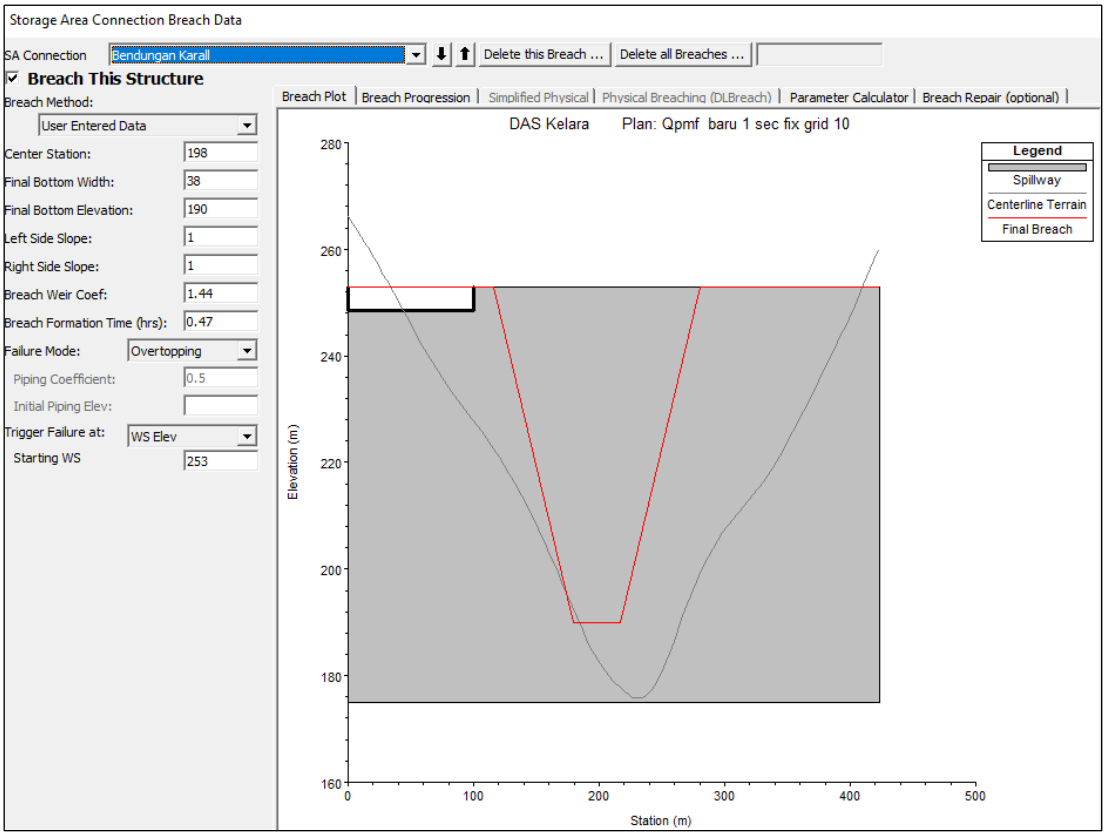

Figure 5. Dam breach parameter plan option is considered a steady Flow

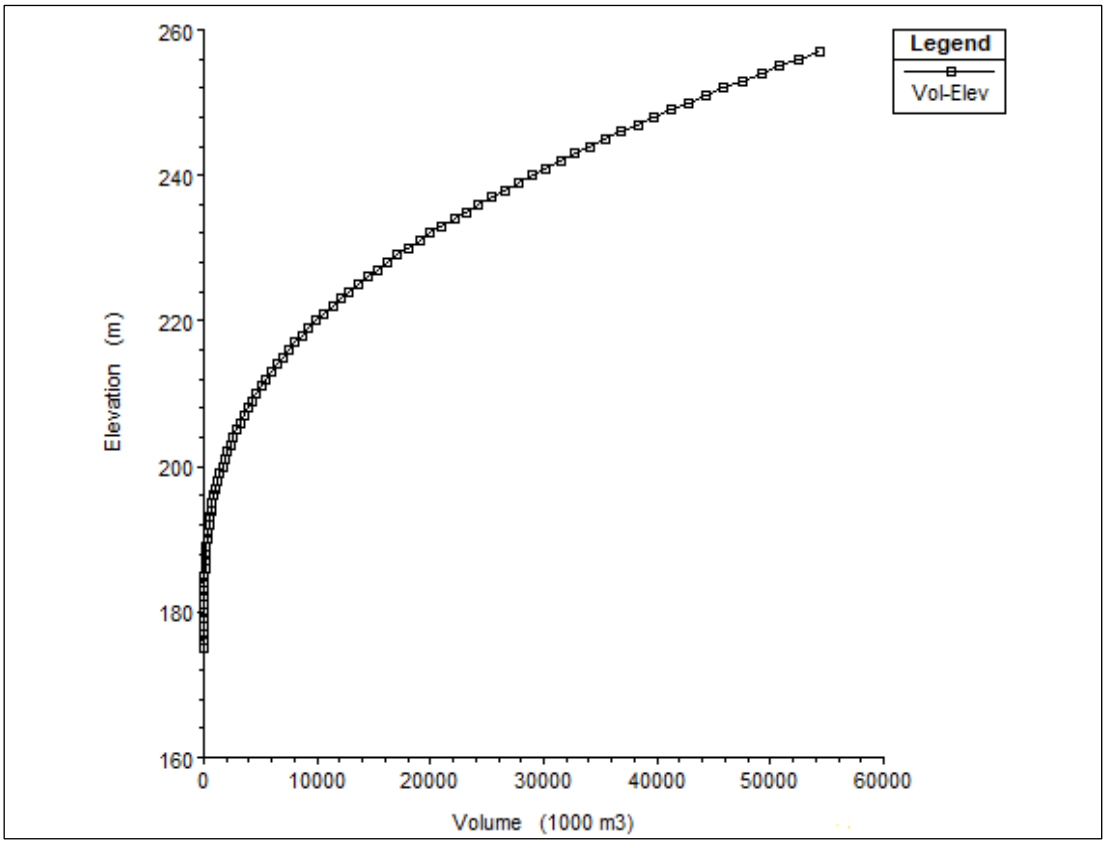

Figure 6. Curve capacity of the Karalloe dam's reservoir

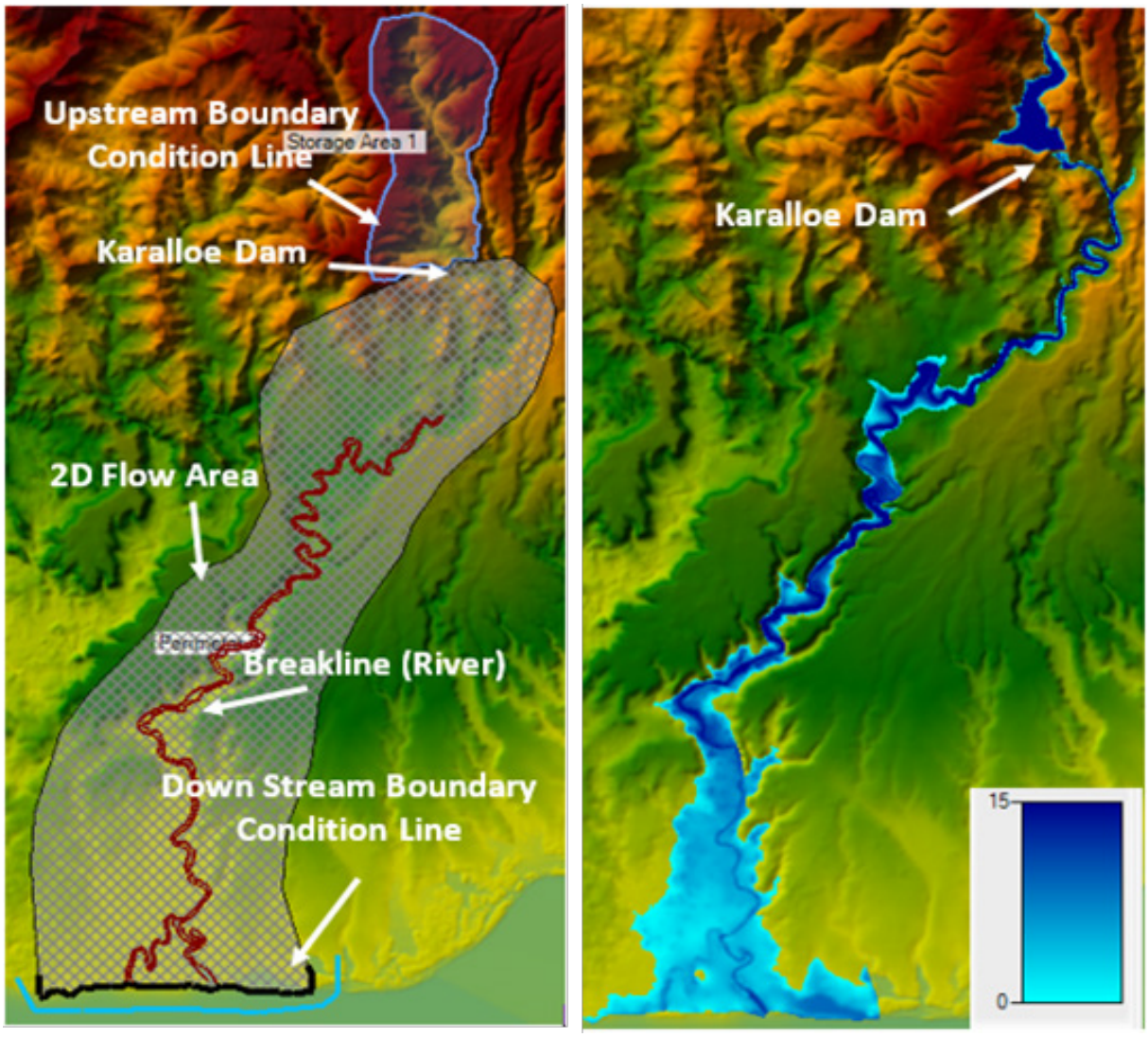

Figure 7. Map of DEM/boundary condition and simulation result of the Karalloe dam's failure

The simulation results of a dam collapse carried out not only produce the distribution of flood inundation but also provide information on the depth at the point to be reviewed, the velocity of the flood flow, and the flood arrival time at a particular location. In general, the flooding visualization due to the collapse of the Karalloe Dam at its top condition can be seen in Figure 7.

The Karalloe dam failure simulation results show that the dam collapsed at 2:28:01 with a QPMF discharge of 3534.8 m^3/s (simulation time). The floodwater depth level downstream of the Karalloe Dam has decreased as the distance travelled and the time for the flood has increased.

3.3. Affected Area and Population

A flood hazard map was created as a reference based on the simulation results of the Karalloe dam's failure to determine the extent of the flood impact caused by the dam's collapse. The flood hazard map is intended to provide information on areas that will be flooded due to a dam failure. The local government and dam managers can coordinate the notification (warning) process for residents and evacuation procedures for residents who are at risk based on this flood hazard map. Figure 8 depicts the area affected by the collapse of the Karalloe Dam in greater detail.

Figure 8 shows that the collapse of the Karalloe Dam has affected 22 villages from 5 sub-districts. Table 4 shows the affected areas in greater detail. Aside from flood-prone maps, simulation results can also provide information on how long it takes floods to reach each area based on distance and topographical conditions. Monitoring points in densely populated areas must be established to provide information on flood travel times and increase community preparedness in a dam emergency to mitigate the impact of the Karalloe dam's collapse. For more information, see Figure 9 and Table 5. They show flood tracking in the affected areas.

According to Table 5, the arrival time of flooding to residential areas, namely the fastest standby time, is within

12 minutes at Lookout Point 7 in Paitana Village. Furthermore, the longest time is 1 hour and 57 minutes at Lookout Point 22 in Paitana Village. This information is critical for the local government in developing a rescue plan for the people affected by the Karalloe dam failure.

Table 3. Maximum Daily Rainfall from TRMM posts

Year	Maximum Daily Rainfall (mm)		
	Pos 1	Pos 2	Pos 3
1998	87	64	80
1999	128	137	173
2000	108	112	96
2001	95	99	98
2002	75	75	83
2003	96	87	88
2004	102	103	96
2005	85	71	77
2006	129	123	97
2007	73	79	72
2008	72	72	96
2009	84	89	80
2010	111	134	101
2011	84	87	94
2012	70	73	81
2013	108	118	155
2014	74	79	96
2015	116	113	138
2016	80	82	101
2017	95	100	102
2018	80	76	78
2019	109	127	138
2020	89	100	74

3.4. Discussion

Dams currently provide numerous agricultural, social, and economic benefits, making dams an extremely vital infrastructure. Dams have also played an essential role in protecting human floodplain settlements [24]. Similarly, the Karalloe Dam serves an essential purpose for the surrounding community. Dams are critical in protecting against flood hazards because of extreme events such as the Lanina effect and uncontrolled population growth in flood-prone areas [25]. The results of this study, however, show that a dam collapse can generate a flood wave that is significantly larger in terms of volume released and velocity of the water generated than a natural-induced flood wave. This condition can cause more severe economic damage and casualties [26]. As a result, it is critical to conduct a complex and in-depth study of the dam collapse to provide an overview to the communities downstream of the dam about the impact and implement strategies to reduce the risks that may occur. The findings of this study should be used to develop mitigation strategies for watersheds with dams, such as the Karalloe Dam in Gowa Regency.

Table 4. Areas affected by flooding due to Karalloe dam collapse

Affected areas		
Village	Districts	Regency
Taring	Biringbulu	Gowa
Garing	Biringbulu	Gowa
Tolo Utara	Kelara	Jeneponto
Tolo	Kelara	Jeneponto
Paitana	Turatea	Jeneponto
Parangloe	Biringbulu	Gowa
Mangepong	Turatea	Jeneponto
Langkura	Turatea	Jeneponto
Bonto Mate'ne	Turatea	Jeneponto
Tanjonga	Turatea	Jeneponto
Kayuloe Barat	Turatea	Jeneponto
Jombe	Turatea	Jeneponto
Sapanang	Binamu	Jeneponto
Empoang Utara	Binamu	Jeneponto
Balang	Binamu	Jeneponto
Balang Toa	Binamu	Jeneponto
Empoang	Binamu	Jeneponto
Sidenre	Binamu	Jeneponto
Monro - Monro	Binamu	Jeneponto
Empoang Selatan	Binamu	Jeneponto
Panaikang	Binamu	Jeneponto
Pabiringa	Binamu	Jeneponto

Table 5. Flood travel time due to the collapse of the Karalloe dam

Code	Coordinates	Location	Distance from the dam (Kilometers)	Flood arrival time (minutes)
Lookout Point 1	5°31'28.79"LS & 119°48'56.18"E	Tolo Utara Village, Kelara District, Jeneponto Regency	1.903	17
Lookout Point 2	5°33'15.68"LS & 119°48'0.13"E	Taring Village, Biringbulu District, Gowa Regency	8.026	26
Lookout Point 3	5°33'25.20"LS & 119°47'35.77"E	Taring Village, Biringbulu District, Gowa Regency	8.874	32
Lookout Point 4	5°34'14.46"LS & 119°46'50.66"E	Paitana Village, Turatea District, Jeneponto Regency	11.463	35
Lookout Point 5	5°33'44.42"LS & 119°46'31.80"E	Parangloe Village, Biringbulu District, Gowa Regency	12.855	40
Lookout Point 6	5°34'45.73"LS & 119°46'1.55"E	Mangepong Village, Turatea District, Jeneponto Regency	16.057	32
Lookout Point 7	5°34'55.27"LS & 119°46'8.12"E	Paitana Village, Turatea District, Jeneponto Regency	16.409	12
Lookout Point 8	5°35'13.26"LS & 119°46'3.36"E	Mangepong Village, Turatea District, Jeneponto Regency	17.628	32
Lookout Point 9	5°36'20.50"LS & 119°45'20.81"E	Bonto Mate'ne Village, Turatea District, Jeneponto Regency	22.620	41
Lookout Point 10	5°36'50.12"LS & 119°45'17.38"E	Bonto Mate'ne Village, Turatea District, Jeneponto Regency	23.853	43
Lookout Point 11	5°37'34.48"LS & 119°44'20.07"E	Jombe Village, Turatea District, Jeneponto Regency	27.114	52
Lookout Point 12	5°37'50.66"LS & 119°44'19.75"E	Kayuloe Village, Turatea District, Jeneponto Regency	27.507	54
Lookout Point 13	5°37'51.00"LS & 119°43'47.13"E	Jombe Village, Turatea District, Jeneponto Regency	28.333	55
Lookout Point 14	5°38'7.01"LS & 119°43'32.05"E	Sapanang Village, Binamu District, Jeneponto Regency	28.886	61
Lookout Point 15	5°38'37.83"LS & 119°44'8.01"E	Sapanang Village, Binamu District, Jeneponto Regency	30.339	63
Lookout Point 16	5°39'2.95"LS & 119°44'31.24"E	Empoang Utara Village, Binamu District, Jeneponto Regency	31.564	67
Lookout Point 17	5°39'11.32"LS & 119°44'14.44"E	Sapanang Village, Binamu District, Jeneponto Regency	31.802	70
Lookout Point 18	5°39'47.04"LS & 119°44'7.35"E	Balang Village, Binamu District, Jeneponto Regency	33.227	76
Lookout Point 19	5°39'55.44"LS & 119°44'26.34"E	Empoang Utara Village, Binamu District, Jeneponto Regency	33.831	78
Lookout Point 20	5°40'42.15"LS & 119°44'33.74"E	Balang Toa Village, Binamu District, Jeneponto Regency	35.615	83
Lookout Point 21	5°40'56.76"LS & 119°44'6.81"E	Balang Toa Village, Binamu District, Jeneponto Regency	36.860	97
Lookout Point 22	5°41'30.63"LS & 119°43'33.45"E	Pabiringa Village, Binamu District, Jeneponto Regency	39.743	117
Lookout Point 23	5°41'14.98"LS & 119°44'35.16"E	Sidenre Village, Binamu District, Jeneponto Regency	37.704	98
Lookout Point 24	5°41'34.50"LS & 119°44'18.23"E	Monro - Monro Village, Binamu District, Jeneponto Regency	38.511	105

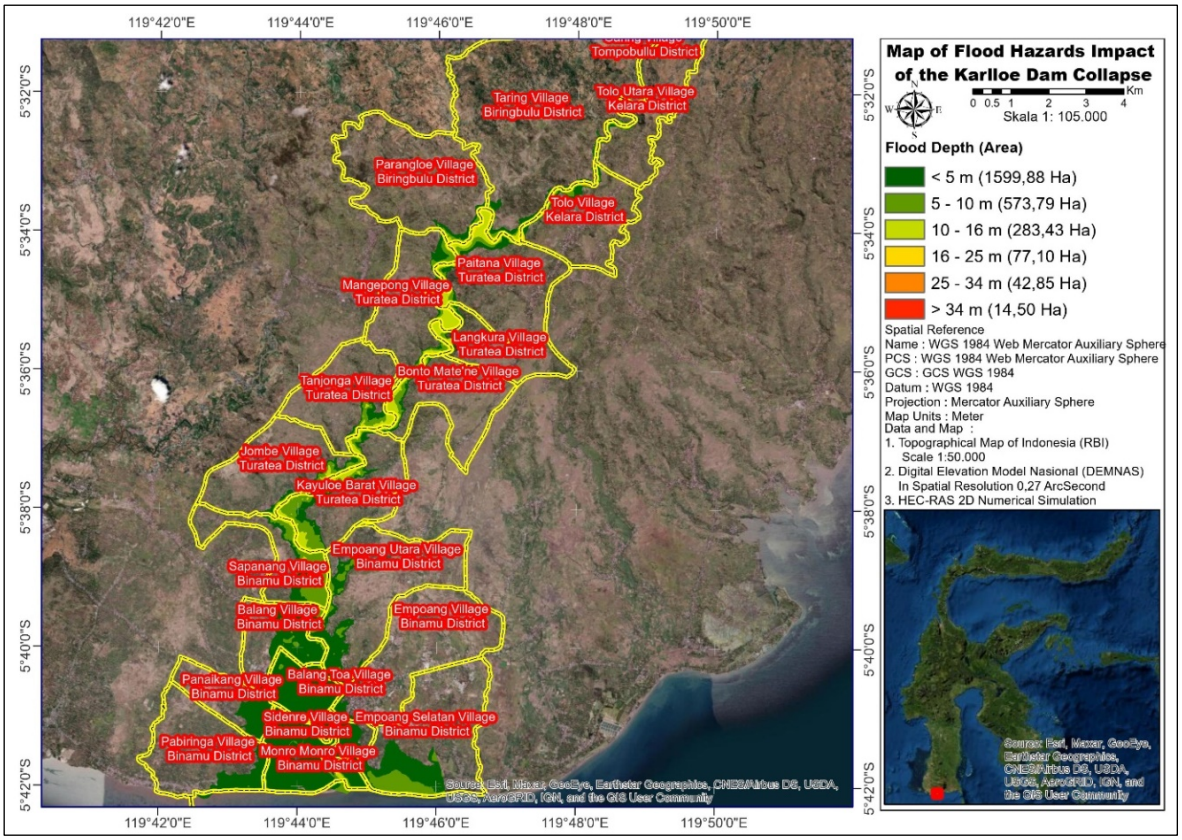

Figure 8. Map of flood hazards due to the collapse of the Karalloe dam

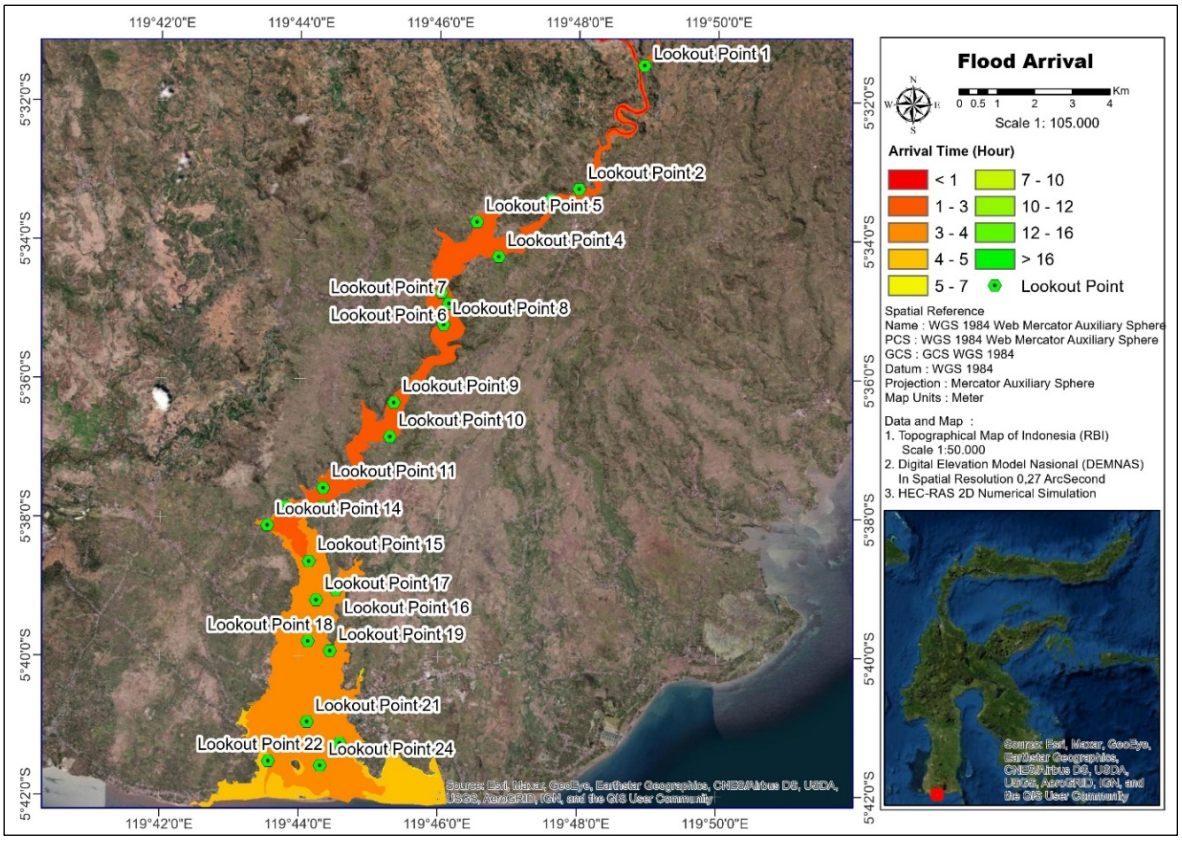

Figure 9. Map of Flood arrival time

The study analysis results found a 63.71% increase in planned discharge from 2012 to 2017 and a 6.9% increase from 2017 to 2021. This rise was caused by an increase in annual rainfall intensity and a rapid land clearing process. The main reason for the need for a dam collapse analysis is to develop a mitigation strategy to reduce losses in a dam failure. Dam failure is known to occur due to overtopping or piping failure. Overtopping refers to the elevation of the water level upstream of the dam that exceeds the elevation of the crest, causing the water to flow over the dam's crest, whereas piping refers to the condition of river water being blocked by the dam and unable to flow into the ground along the base and walls of the natural dam. The most likely outcome in the case of the Karalloe Dam with a type of rock fill with a concrete membrane is dam collapse due to overtopping. According to the simulation, with a discharge of QPMF = 3543 m^3/s on the Karalloe dam, it only takes 2 hours and 28 minutes to go from average to overtopping conditions, and due to the dam's collapse, there are 22 villages from 5 affected districts, namely Taring, Garing, North Tolo, Tolo, Paitana, Parangloe, Mangepong, Langkura, Bonto Mate'ne, Tanjonga, West Kayuloe, Jombe, Sapanang, North Empoang, Balang, Balang Toa, Empoang, Sidenre, Monro – Monro, South Empoang, Panaikang and Pabiringa. The simulation results can determine when the flood reaches the residential location, which can then be used to develop an early warning system for flood hazards. The simulation results also show that the distance from the dam and the topographical conditions of each settlement influence the time it takes for the flood to reach the residential location. Based on the findings of this analysis, 24 monitoring points can be established in densely populated areas, with the fastest time being at monitoring point 7 in Paitana Village, which is 16.4 km from the dam and has a time of 12 minutes. Furthermore, the longest time was recorded at monitoring point 22 in Pabiringa Village, 39,743 km from the dam. This outcome is expected to become a standard operating procedure (SOP) for dealing with flood hazards, allowing downstream communities to anticipate and evacuate to areas that are not flood-prone to minimize flood losses caused by the dam's collapse.

Several previous researchers have also conducted similar studies. For example, Shahrim and Ros [27] emphasize the comparison of 1D and 2D models in dam failure simulations, as well as the comparison of flood arrival time, depth, and velocity due to piping and overtopping, and show that dam failure due to overtopping has higher depth and velocity values than piping. Murdiani et al. [28] also used national digital elevation model data in a 2D simulation, with the results providing an overview of the affected areas and the time of arrival of floods in each village. This previous study is similar to the current research but differs in the effort to improve the model's accuracy, whereas in this study, data from measurements of riverbeds and reservoirs on the dam and monitoring points were used to mitigate the dam's collapse. The findings of this study show that 22 villages along 22 km of riverbank affected, and the present study will assist authorities in developing emergency response plans and preparing guidelines for flood mitigation plans in the research area.

4. Conclusions

Based on the findings of this study, it is possible to conclude that the analysis of flood discharge using the HSS SCS method (i.e., HEC-HMS) with a PMF return period (likely maximum flood) yielded a peak discharge Q inflow of 3534.8 m^3/s. This analysis produced a QPMF value more significant than the designed PMF value of Karalloe Dam, which was 2020 m^3/s in 2012, and the results of other researchers, who produced a QPMF of 3307 m^3/s in 2017. The map of flood-prone areas obtained in this study shows that 22 villages from 5 sub-districts have been affected by the collapse of the Karalloe Dam, namely: the villages of Parangloe, Taring, Garing, Monro, Pabiringa, Panaikang, Epoang Selatan, Balang Toa, Balang, Empoang, Empoang Utara, Sapanang, Kayuloe Barat, Jombe. The collapse occurred at 2:28:01 according to the flood simulation results using HEC-RAS, which is simulated using the QPMF value (simulation time). The floodwater depth level downstream of the Karalloe dam has decreased as the distance traveled and the time for the flood has increased. There are 24 monitoring points planned in densely populated areas affected by the dam collapse to provide information on flood travel times and time to improve community preparedness in an emergency condition at the dam. According to the analysis results, the quickest standby time is at Lookout Point 7 in Paitana Village within 12 minutes, while the longest time is at Lookout Point 22 in Paitana Village within 1 hour 57 minutes. Therefore, the method proposed in this study yields significant results for describing the potential for flooding caused by dam failure. It assists stakeholders in developing disaster prevention policies and provides new insights into the development of disaster prevention technologies, particularly flood prevention technologies.

Acknowledgments

The authors wish to thank the head of Civil Engineering Department of Hasanuddin University for supporting this research. We also gratefully acknowledge the suggestions of anonymous reviewers. This research did not receive any specific grant from funding agencies in the public, commercial, or not-for-profit sectors.

REFERENCES

[1] de Paiva, Camilla A., Aníbal da Fonseca S,, and José F. P. F., "Content analysis of dam break studies for tailings dams

with high damage potential in the Quadrilátero Ferrífero, Minas Gerais: technical weaknesses and proposals for improvements," Natural Hazards, vol. 104, no. 2, pp. 1141-1156, 2020, DOI: 10.1007/s11069-020-04254-8.

[2] Aureli F., Andrea M., Gabriella P., "Review of Historical Dam-Break Events and Laboratory Tests on Real Topography for the Validation of Numerical Models," Water, vol. 13, no. 14, 2021. DOI: 10.3390/w13141968.

[3] Hasbi M., Mappanyompa M., Bakri B., "The construction of Karalloe multipurpose dam for the Kellara technical irrigation development," IOP Conference Series: Earth and Environmental Science, vol. 419, No. 1, IOP Publishing, 2020.

[4] Rakhim, A., Sirajuddin, A., "Evaluation of technical planning and stability analysis of the construction of the Karalloe dam body". Teknik Hidro, vol. 13, no. 1, pp. 18-27, 2020. DOI: 10.26618/th.v13i1.3979. (In Indonesian)

[5] Sandi, R., Rasyidi, E. S., and Fikruddin, M., "Landslide Of Karalloe Dam Site Gowa Regency, South Sulawesi Province," Jurnal Ilmiah Ecosystem, vol. 20, no. 1, pp. 34-40, 2020.

[6] Evangelista S., Altinakar M. S., Di Cristo C., Leopardi A., "Simulation of dam-break waves on movable beds using a multi-stage centered scheme," International Journal of Sediment Research, vol. 28, no. 3, pp. 269-284, 2013. DOI: 10.1016/S1001-6279(13)60039-6.

[7] Kyaw P. P. S. S., "Modeling approach for Earthen dam breach analysis in North Yamar dam, Myanmar," American Academic Scientific Research Journal for Engineering, Technology, and Sciences, vol. 69, no. 1, pp. 59-72, 2020.

[8] Urzică A., Mihu-Pintilie A., Stoleriu C. C., Cîmpianu C. I., Huţanu E., Pricop C. I., Grozavu A., "Using 2D HEC-RAS Modeling And Embankment Dam Break Scenario for Assessing the Flood Control Capacity of A Multi-Reservoir System (NE Romania)," Water, vol. 13, no. 1, 2020. DOI: 10.3390/w13010057.

[9] Perera D., Smakhtin V., Williams S., North T., Curry A., "Ageing Water Storage Infrastructure: An Emerging Global Risk," UNU-INWEH Report Series, vol, 11, 2021.

[10] Bocchiola D., Renzo R., "Safety of Italian Dams in the Face of Flood Hazard," Advances in water resources, vol. 71, pp. 23-31, 2014. DOI: 10.1016/j.advwatres.2014.05.006.

[11] Krztoń W., Walusiak E., Wilk-Woźniak E., "Possible Consequences of Climate Change on Global Water Resources Stored in Dam Reservoirs," Science of The Total Environment, vol. 830, 2022. DOI: 10.1016/j.scitotenv.2022.154646.

[12] Li Z., Li W., Ge W., "Weight Analysis of Influencing Factors of Dam Break Risk Consequences," Natural Hazards and Earth System Sciences, vol. 18, no. 12, pp. 3355-3362, 2018. DOI: 10.5194/nhess-18-3355-2018.

[13] Ahmadi S. M., Yoshimichi Y., "A New Dam-Break Outflow-Rate Concept and Its Installation to a Hydro-Morphodynamics Simulation Model Based on FDM (An Example on Amagase Dam of Japan)," Water, vol. 13, no. 13, 2021. DOI: 10.3390/w13131759.

[14] Said N. F. M., Mohd Sidek L., Mustafa Z., Mansor F. H., Jamal M., "Emergency Action Plan for Public Safety Around the Juaseh Dam, Johor," International Conference on Dam Safety Management and Engineering, Springer, Singapore, 2019. DOI: 10.1007/978-981-15-1971-0_11.

[15] Azeez O., Elfeki A., Kamis A. S., Chaabani A., "Dam Break Analysis and Flood Disaster Simulation in Arid Urban Environment: The Um Al-Khair Dam Case Study, Jeddah, Saudi Arabia," Natural Hazards, vol. 100, no. 3, pp. 995-1011, 2020. DOI: 10.1007/s11069-019-03836-5.

[16] Kheirkhah G. H., Halliday A., Arenas A., Zhang H., "Tailings Dam Breach Analysis: A Review of Methods, Practices, And Uncertainties," Mine Water and the Environment, vol. 40, no. 1, pp. 128-150, 2021. DOI: 10.1007/s10230-020-00718-2.

[17] Nazif H. M., "Advance Mosul Dam Break Analysis by Integrated Hydrologic Modeling and Gene-Expression Programming," Zanco Journal of Pure and Applied Sciences, vol. 31, no. 3, pp. 423-429, 2019.

[18] Kilania S., Chahar B. R.,"A Dam Break Analysis Using HeC-RAs," World Environmental and Water Resources Congress 2019: Hydraulics, Waterways, and Water Distribution Systems Analysis. Reston, VA: American Society of Civil Engineers, 2019.

[19] Bharath A., Shivapur A. V., Hiremath C. G., Maddamsetty R., "Dam break analysis using HEC-RAS and HEC-GeoRAS: A case study of Hidkal dam, Karnataka state, India." Environmental Challenges, vol. 5, 2021, DOI: /10.1016/j.envc.2021.100401.

[20] Karamma R., Pallu M. S., "Comparison of Model Hidrograf Synthetic Units (HSS) with the Model of Hidrograf Observations on DAS Jeneberang Gowa Regency, Indonesia," International Journal of Innovative Science and Research Technology, vol. 3, no. 2, pp. 617-623, 2018.

[21] Mustamin M. R., Maricar F., Karamma R., "Hydrological Analysis in Selecting Flood Discharge Method in Watershed Of Kelara River," INTEK: Jurnal Penelitian, vol. 8. no. 2, pp. 141-150, 2021. DOI: 10.31963/intek.v8i2.2874.

[22] Vernimmen R. R. E., Hooijer A., Aldrian E., Van Dijk A. I. J. M., "Evaluation and Bias Correction of Satellite Rainfall Data for Drought Monitoring in Indonesia," Hydrology and Earth System Sciences, vol. 16, no. 1, pp. 133-146, 2012. DOI: 10.5194/hess-16-133-2012, 2012.

[23] Froehlich D. C., "Peak Flood Discharge from a Landslide Dam Outburst," Natural Hazards Review, vol. 23, no.2, 2022. DOI: 10.1061/(ASCE)NH.1527-6996.0000545.

[24] Romanescu G., Stoleriu C. C., "Exceptional Floods in the Prut Basin, Romania, in the Context of Heavy Rains in the Summer of 2010," Natural Hazards and Earth System Sciences, vol. 17, no. 3, pp. 381-396, 2017. DOI: 10.5194/nhess-17-381-2017.

[25] Mihu-Pintilie A., Cîmpianu C. I., Stoleriu C. C., Pérez M. N., Paveluc L. E., "Using High-Density LiDAR Data and 2D Streamflow Hydraulic Modeling to Improve Urban Flood Hazard Maps: A HEC-RAS Multi-Scenario Approach," Water, vol. 11, no. 9, pp. 1832, 2019. DOI: 10.3390/w11091832.

[26] Lukman S., Otun J. A., Adie D. B., Ismail A., Oke I. A., "A Brief Assessment of a Dam and its Failure Prevention,"

Journal of Failure Analysis and Prevention, vol. 11, no. 2, pp. 97-109, 2011. DOI: 10.1007/s11668-010-9420-1.

[27] Shahrim M. F., Ros F. C., "Dam Break Analysis of Temenggor Dam using HEC-RAS," IOP Conference Series: Earth and Environmental Science. Vol. 479. No. 1. IOP Publishing, 2020.

[28] Murdiani K. M., Sangkawati S., Sadono K. W., "Dam Collapse Modeling using HEC-RAS 2D Case Study of Gondang Dam, Karanganyar Regency," Rekayasa, vol. 13, no. 2, pp. 205-211, 2020. DOI: 10.21107/rekayasa.v13i2.6872.